RSC Applied Interfaces

ROYAL SOCIETY OF CHEMISTRY

PERSPECTIVE

View Article Online
View Journal | View Issue

Cite this: *RSC Appl. Interfaces*, 2024, **1**, 70

The role of ceria/precious metal interfaces in catalysis

Michele Melchionna *[a] and Paolo Fornasiero *[ab]

Received 18th October 2023,
Accepted 27th November 2023

DOI: 10.1039/d3lf00202k

rsc.li/RSCApplInter

The popularity of ceria (CeO_2) supports has been increasing over the last three decades on account of the rich redox chemistry of such an oxide. The ability to act as an oxygen buffer and switch the oxidation state of Ce depending on conditions implies that the role of this oxide goes beyond the conventional function of stabilizing nanoparticles. In fact, ceria can actively participate in catalytic reactions by interacting with the supported metal, in particular precious metals, promoting various types of dynamic processes that are beneficial for catalysis. This perspective put into light such interfacial synergy, and the effects in several catalytic processes, encompassing the most traditional applications up to the most modern reaction schemes.

Introduction

Precious metals (PMs) and cerium dioxide (also known as "ceria", CeO_2) have been sharing a long relationship in the history of heterogeneous catalysis. This is explained by the successful combination of their properties that made many catalytic conversions with high efficiency feasible. Much of the initial interest, which dates back to at least six decades ago, was derived from the knowledge that some metal oxides (*e.g.* zirconia, thoria *etc.*) are excellent oxygen carriers. Such a property could be exploited to promote the catalytic activity of noble metals in important reactions, such as hydrogenation of olefins.[1] Continuing evidence of some metal oxide effects led to the terminology "active supports" to define metal oxides such as CeO_2, alternatively referred to as "promoters" or "non-innocent supports". In the 1980s, the literature on the specific PM–CeO_2 interaction started to appear, focusing in particular on Pt as the PM, mainly reporting the oxygen (or other gases) adsorption behaviour of Pt nanoparticles deposited on ceria.[2] Other probe molecules such as H_2 or CO were lately investigated in-depth, as they represent typical reactants for the most studied catalytic processes. Defining a paradigm of the adsorption behaviour in the framework of PM/CeO_2 composites has been highly challenging, and not yet fully achieved, on account of the high adsorption capacity of CeO_2 towards H_2 and CO, which makes it difficult to discriminate between metal and metal support contributions.

[a] *Department of Chemical and Pharmaceutical Sciences, Center for Energy, Environment and Transport "Giacomo Ciamician", INSTM UdR Trieste, University of Trieste, Via Licio Giorgieri 1, 34127 Trieste, Italy.*
E-mail: melchionnam@units.it, pfornasiero@units.it
[b] *ICCOM-CNR, Unit of Trieste, Italy*

The initial strongest driving force for research on Pt/CeO_2 was related to the needs of the automotive exhaust industry, where emission control in three-way catalysts heavily depended on the use and improvement of catalysts integrating Pt/CeO_2.[3] Our research group has been contributing to this topic for several years and with growing enthusiasm,[4] and it became evident that the effects of ceria as a promoter for PM nanoparticles went beyond the mere stabilization and dispersion of the NP, but it involved an improved functionality of the PM/CeO_2 system. Of utmost importance, the reducibility of CeO_2 harnesses the release of active oxygen so that the support actively participates in the catalytic cycle.[5] It has been demonstrated that for many reactions the catalytic site is located at the interface of PM NPs and CeO_2,[6] where synergy is maximum, and this led to synthetic efforts aiming at the maximization of the interfacial area. This perspective article illustrates some of the most meaningful work that over the years contributed to shedding light on the role of interfaces in PM NPs supported on CeO_2 for various catalytic processes.

Seminal works on thermal catalysis by PM/CeO_2

One of our seminal studies showed that the supramolecular-inspired assembly of Pd/CeO_2 nanoparticles with a precise core–shell configuration allowed almost complete methane oxidation conversions to be reached at a lower temperature (400 °C) (Fig. 1), surpassing the performance of what at that time were the state-of-the-art catalysts.[7]

This work gives a clear demonstration of how assembling structures with a controlled hierarchy impacts to a large extent the properties of the catalytic system. In the above specific case, the core–shell hierarchy provides extra stability for the Pd NPs, avoiding their sintering at high temperature,

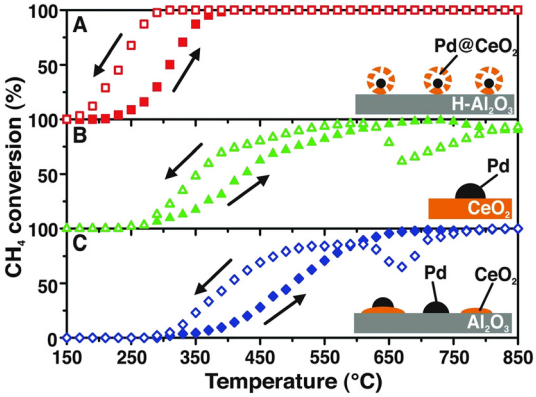

Fig. 1 Heating and cooling during CH_4 conversion for: A) Pd@CeO_2/hydrophobic Al_2O_3 (H-Al_2O_3) core–shell catalyst; B) Pd/CeO_2 prepared by incipient wetness impregnation, and C) Pd/CeO_2/Al_2O_3 prepared by coimpregnation of Pd and Ce precursors. Reproduced from ref. 7 with permission from AAAS, copyright 2012.

and the activity benefits from the extended Pd–CeO_2 interaction. Optimisation of the oxide–metal interaction is a key factor for maximising catalytic performance, and a number of strategies have been proposed.[8]

As hinted earlier, the oxygen buffer functionality of CeO_2 is dependent on its defectivity, and within this framework the role of oxygen vacancies is known to be the most critical. However, in contrast with the majority of metal oxides such as TiO_2, where vacancy formation is instrumental to create binding sites within the structure, in the case of ceria the results of oxygen removal are accompanied by significant electronic changes. In particular, the presence of empty f orbitals on Ce results in a localization of the excess electron that caused change in the valence state of Ce^{4+} to Ce^{3+} of the two Ce centres adjacent to the vacancy. It turns out that thorough knowledge of the oxygen vacancy formation, type and distribution is of high relevance to predict CeO_2 catalytic behaviour and appropriately design PM/CeO_2 catalysts. To this end, scanning tunnelling microscopy (STM) has proven to be a powerful tool for understanding the details of vacancy formation, and the evolution of the CeO_2 surface and subsurface in terms of electron localization, valence states and the coordinative surrounding of the Ce cationic species.[9] Based on the observed synergy between PM and CeO_2 for several catalytic processes, intensive research on the exploitation of such an interaction has been proliferating over the years. The so-called "strong metal–support interaction" (SMSI) coined by Tauster *et al.* to describe the significant detrimental effects of the TiO_2 support on the H_2 and CO chemisorption properties of Pt NPs[10] was reanalysed in the case of Pt/CeO_2 to explain how this interaction differs and resulted in enhanced catalytic performance. Sanchez and Gazquez modelled the SMSI for fluorite-type supports such as CeO_2 and compared it to that observed in rutile supports, observing a remarkably different behaviour of the supported PM NP in terms of stability and catalytic activity. In fact, they noticed that the CeO_2 type of structure presents a cationic sub-lattice structure able to create a diffusion barrier for the metal, preventing its penetration into the bulk, in contrast with rutile-type structures. This feature is one of the descriptors for explaining the catalytically beneficial SMSI effect of PM/CeO_2 catalysts.[11] Moreover, experiments for the characterization of PM/CeO_2 conducted under reducing conditions with H_2 flows could be set at temperatures higher than 773 K, an upper limit typically dictated by the TiO_2 support. This possibility allowed a better understanding of the nature of the metal/support interaction to be obtained, and Bernal *et al.* reported several detailed investigations by means of high-resolution electron microscopy (HREM) of the structural evolutions of PM/CeO_2 under both high temperature reducing and oxidizing conditions. A remarkable difference is that, in contrast to PM/TiO_2 systems, the high temperature H_2 treatment does not cause covering of the metal microcrystal by the reduced support (Fig. 2).[12]

Inspired by Frost's junction effect theory,[13] Acerbi *et al.* first put into relation the reducibility of ceria with the work function of various precious metals such as Au, Ag, Pd, Pt, Rh, Ru to rationalize the different SMSIs.[14] However, the same authors later claimed that relationship with the d-band centres of the precious metals was a better descriptor of the SMSI as it provides a more satisfactory correlation of the ceria H_2 chemisorption with the PM electronic structure.[15] The SMSI has been fruitfully exploited in applications such as thermal hydrogenation reactions: in a seminal work, Trovarelli *et al.* described the use of transient and steady-state thermal hydrogenation of CO and CO_2 by Rh/CeO_2, which could reveal the effect of the metal–metal oxide support,[16] while in another article the importance of the generated bulk vacancies on ceria by means of reduction at high temperatures was discussed.[17] More recently, the selective hydrogenation of CO_2 to CO, avoiding methanation, was achieved by tuning the chemical state of Ir species supported on CeO_2, with the SMSI effect being critical for controlling efficiently the Ir chemical state.[18] Hydrogenation of phenol to cyclohexanone at room temperature was achieved by using Pd/CeO_2, thanks to the ability of CeO_2 to chemisorb phenoxy species and facilitate attack by Pd-activated hydrogen.[19]

Campbell *et al.* introduced the term "electronic metal–support interaction" (EMSI) to better include all the complex and synergistic charge redistributions that were at the origin of improved catalytic performance of PMs and CeO_2.[20] Bruix *et al.* proposed a new type of metal–support interaction for Pt/CeO_2 on the basis of photoemission measurements and DFT calculations while studying the water-gas shift reaction (WGSR). The observed catalytic activity was then related to a dramatic charge distribution occurring for the Pt adatoms on ceria, with favorable Pt → CeO_2 charge transfer and CeO_2 → Pt oxygen transfer. Following this electronic interaction, the adsorption of H_2O on Pt becomes more favourable, and the dissociation of the O–H of water becomes a very exothermic process, enhancing H_2 evolution (Fig. 3).[21]

Nevertheless, this type of electronic metal–support interaction is also linked to the size of the metal NP. A

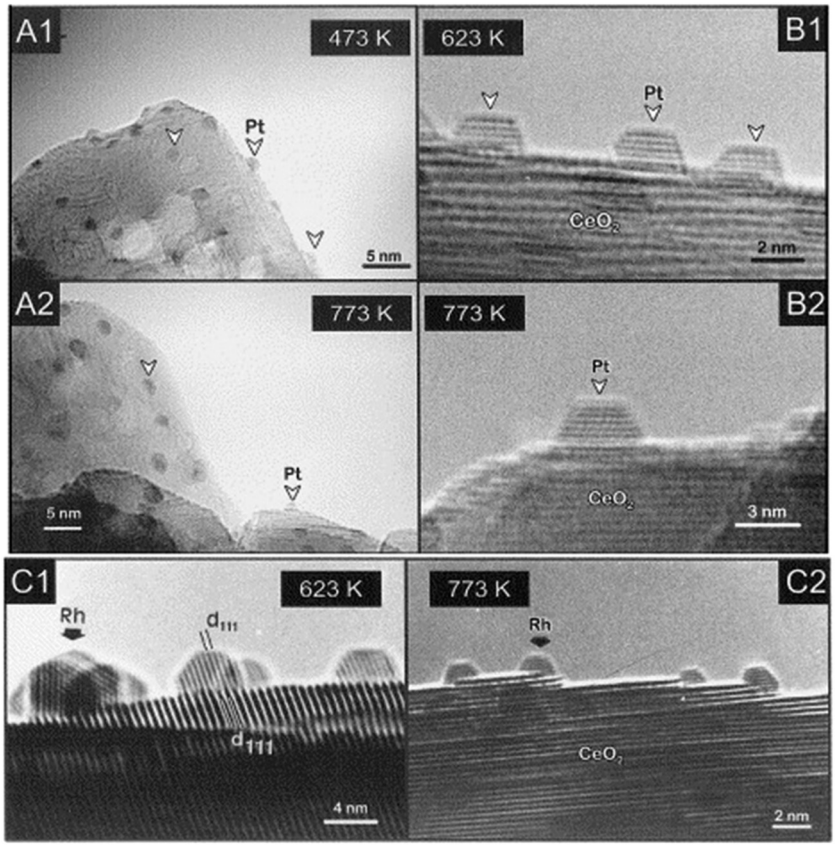

Fig. 2 HREM images of various CeO_2-supported Pt and Rh catalysts reduced with H_2 at different temperatures. Profile view images corresponding to: (A1–A2) Pt(7%)/CeO_2-MS; (B1–B2) Pt(4%)/CeO_2-LS; (C1–C2) Rh(2.4%)/CeO_2-LS (MS and LS denotes two different ceria samples). Reproduced from ref. 12*c* with permission from Elsevier, copyright 1999.

quantitative analysis of the charge transfer occurring between Pt and CeO_2 in well-defined composites was performed by a combination of STM, XPS and DFT, unveiling that the EMSI is closely linked to the size of the Pt NPs. The maximum charge transfer occurs for Pt NPs composed of 30 to 70 atoms, while for smaller or larger nanoparticles the charge transfer is hindered either by nucleation at defect sites (smaller NPs) or directly by the support (larger NPs). The result is of relevance for the preparation of optimum PM NP sizes, but it also highlights the dependence of the synergistic effects from subtle structural differences.

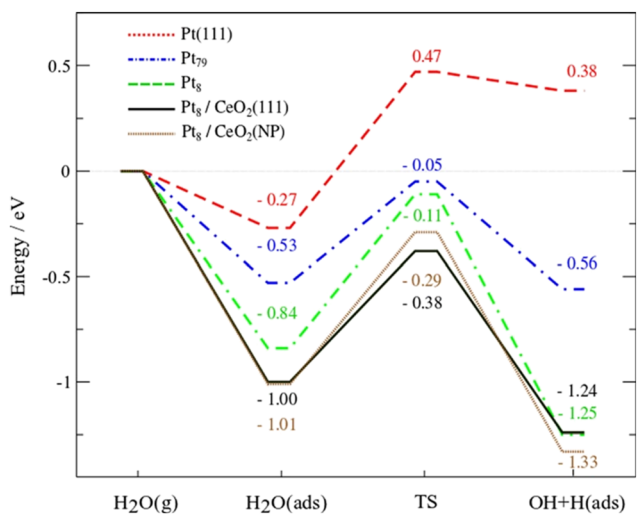

Fig. 3 DFT-calculated energy profiles for the dissociation of water on Pt(111), Pt_{79} and Pt_8 clusters, and Pt_8 on CeO_2(111) or $Ce_{40}O_{80}$ NPs. Reproduced from ref. 17 with permission from American Chemical Society, copyright 2012.

Model catalysts

Given the complexity of the metal–support fundamental phenomena, it became evident that model systems were an inevitable choice for studying ceria–PM interfaces. A large variety of well-defined metal–ceria systems were prepared and investigated in relation to a few specific catalytic processes, such as CO oxidation, CO_2 hydrogenation, WGSR and methane or alcohol reforming. In previous studies, the assembly of such model catalysts was based on synthetic routes (deposition of metallic Ce followed by oxidation, or oxidation of metal–Ce alloys) that could not establish a perfect control of the structural order.[22] More recently, controlled growth of CeO_2 nanoparticles could be achieved *via* epitaxy and the ceria phase structure and composition can be accurately controlled by means of post-growth thermal

treatments.[23] Rodriguez *et al.* provided a comprehensive review on the most important aspects that are involved in the design, synthesis and characterization of metal–ceria model catalysts, emphasizing the strong dependence of the catalytic activity from a large number of variables, which have to be controlled *ad hoc* for a specific process.[24] It is interesting to note the resorting to inverse model catalysts, where the two components (PM and CeO_2) switch roles for a more complete understanding of the functionality of the system and identifying optimum activity conditions. An important advantage of inverse model catalysts lies in the possibility to unravel novel interfacial effects by means of highly resolved electron-based techniques such as low energy electron microscopy (LEEM) and X-ray photoemission electron microscopy (XPEEM).[25] The spatial resolution of such techniques is compromised on conventional model catalysts because of charging effects occurring on insulating metal oxides during probing, a problem that is alleviated in inverse catalysts where the conducting area is much larger as it is made of metals. This variant has mostly involved the synthesis of CeO_2 nanoparticles grown on (111) facets of metal surfaces, distinguishing the cases of oxidisable, for instance Cu(111) and non-oxidisable metals, such as Au(111) (Fig. 4A).[26] This distinction has been used to determine both the mode of CeO_2 growth and catalytic reaction-relevant phenomena, such as oxygen spillover.[27]

For example, in the oxidation reaction of carbon monoxide ($2CO + O_2 \rightarrow 2CO_2$), the poor interaction and dissociation of O_2 with respect to the Cu(111) surface is significantly improved by the presence of the CeO_2 NP, which spills oxygen to Cu and allows the formation of an oxygen-deficient Cu_2O_{1+x} phase, more active for the oxidation of CO. The details of CeO_2 growth and formation of the new Cu_2O_{1+x} phase could be uncovered thanks to the precise crystalline order of the inverse catalyst and the use of scanning tunnelling microscopy (STM), confirming that the ceria-promoted oxidation of Cu proceeds with the formation of both ordered $Cu_2O(111)$ and Cu_2O_{1+x} (Fig. 4B).[28] Recent studies evaluated the redox phenomena occurring at the Pt/CeO_2 interface in inverse model catalysts consisting of epitaxially grown CeO_2 on single crystal Pt(111). Interestingly, the authors could distinguish the different sites where reduced ceria is stabilized by the metal as opposed to sites far away from the Pt.[29]

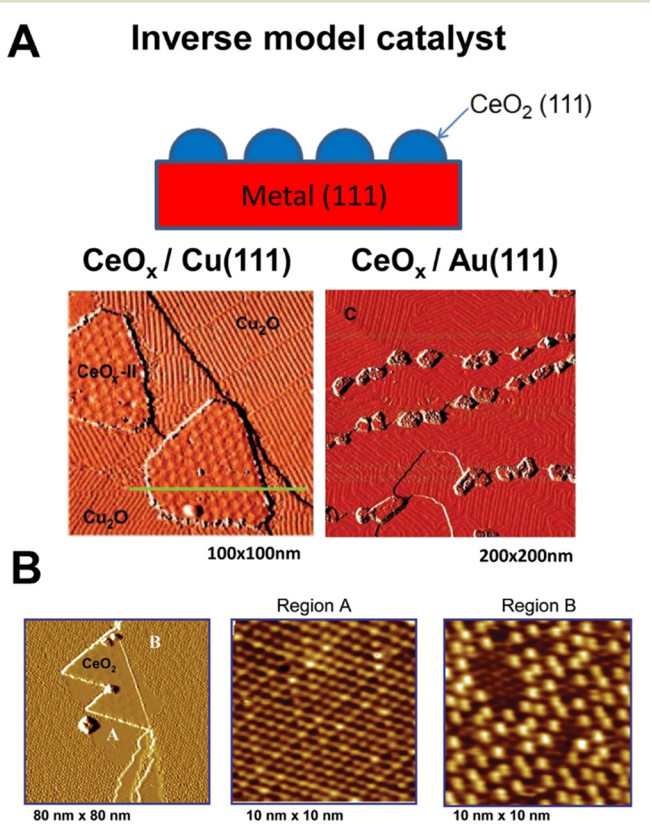

Fig. 4 A) Top: Schematic of an inverse model catalyst; bottom: STM images for inverse $CeO_x/Cu_2O/Cu(111)$ and $CeO_x/Au(111)$ model catalysts; reprinted with permission from ref. 22, copyright 2013 American Chemical Society. B) STM images of ceria promoted surface oxidation of Cu(111); the first panel shows the $CeO_2/Cu(111)$ surface exposed to 5×10^{-7} Torr O_2 at 550 K for 5 min. Reproduced from ref. 24 with permission from American Chemical Society, copyright 2011.

Model catalysts *vs.* bulk catalysts

Despite the atomic scale understanding that model systems offer, such knowledge cannot be straightforwardly transferred to bulk composites prepared by more conventional protocols. In those situations, a combination of a variety of characterization techniques is required to hypothesize and confirm the synergistic properties of metal–ceria. A first consideration relates to the fact that many studies incorporate a third phase in addition to ceria and metals, and in several cases such an extra component may considerably affect the overall properties of ceria and in turn its interfacial dynamics with PM NPs. As our group demonstrated, this situation occurs for example with the incorporation of carbon nanostructures (CNSs) within the nanocomposite. CNSs can often influence the reducibility of CeO_2 and the Ce^{4+}/Ce^{3+} ratio, implying a differential interaction with the metal nanoparticles.[30] Moreover, CeO_2 can be a useful stabilizing phase in Pt/CNS catalysts, as demonstrated during selective glycerol-to-glyceric acid (GLYA) catalytic oxidation by Pt/CNT/CeO_2 (CNT = carbon nanotubes), where ceria improves the anti-poisoning of the Pt nanoparticle by GLYA by modulation of the Pt electronic structure (Fig. 5).[31]

Besides, preparative routes based on conventional methods lead to bulk materials with important sample inhomogeneity and at times the presence of unexpected impurities that play a role. Unfortunately, not always all these possibilities are taken into account, which has resulted in the proliferation of articles on Pt/CeO_2 catalysts where support effects and synergy are somehow taken for granted, causing misleading interpretation of results. A seminal article by Fu *et al.* posed critical questions on the contentious identification of the catalytically active sites in PM/CeO_2 used

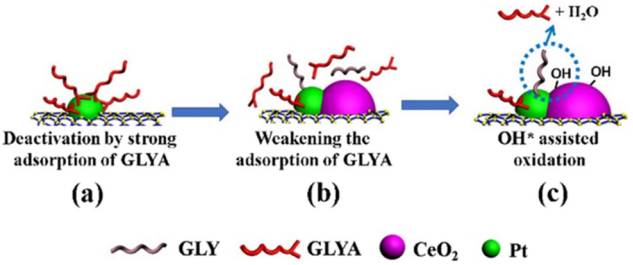

Fig. 5 Proposed mechanisms for overcoming the deactivation of Pt/CNTs by introducing CeO_2. Reproduced from ref. 27 with permission from American Chemical Society, copyright 2020.

in WGSR, CO oxidation and other oxidation; specifically whether these are invariably located at the metal–ceria interface. The investigation focused on Au/CeO_2 and Pt/CeO_2 catalysts for the WGSR, whereby careful analysis on the kinetics of leached and unleached composite catalysts evidenced that the WGSR catalytic activity was not due to interfacial effects. Metallic Au and Pt NPs were ineffective for the catalytic activity, which instead originated from the isolated Au or Pt ions stabilized on CeO_2 through lattice substitution.[32] As a matter of fact, the work represents the first example of single-atom catalysis in the WGSR, which the authors further corroborated in the following studies, highlighting the essential presence of Pt-alkali-$O_x(OH)_y$ species,[33] as well as the fact that the activity is not an exclusiveness of the CeO_2 support.[34] An important contribution into the field of Pt-SAC/CeO_2 was provided by Nie *et al.* who explained how ceria is able to activate atomically dispersed Pt^{2+} metal ions by means of active surface lattice oxygen formed during aging of the catalyst at 750 °C. Hence, the catalytic activity towards CO oxidation was greatly improved without sacrificing the ionic nature of isolated Pt^{2+}, which is generally compromised by the very strong binding of CO molecules to the metal.[35] High activities for the water-promoted CO oxidation by Pt-SAC/CeO_2 were also observed by Wang *et al.*, who found that the lattice hydroxyl species at the interface between Pt and CeO_2 played a critical role in the reaction, yielding the carboxyl reaction intermediate.[36]

Electrocatalytic applications

The examples provided above and the discussion of the growing understanding on PM and CeO_2 interfaces were rightly focused on the most deeply explored thermal catalysis. Nevertheless, researchers soon realized that the synergistic effects had potential for exploitation in other types of catalytic applications. Electrocatalysis gained attention towards the beginning of the 2000's and after that Marina *et al.* fabricated electrodes based on Gd-doped CeO_2/Au NPs for the electrochemical oxidation of methane.[37] While the work did not directly studied the interfacial phenomena occurring at the Au–ceria junction, it triggered successive investigations focused more on the understanding on the promoting role of ceria. Obvious motivations were dictated by the oxygen buffer ability of ceria, which was for instance an advantage for the electrocatalytic oxygen reduction reaction (ORR). In this framework, the facile oxygen adsorption and desorption on the ceria component was recognized to be instrumental in supplying oxygen to the metal NP.[38] However, in most of the examples, PM/CeO_2 is employed as fuel cell-relevant anodic electrocatalysts for the oxidation of fuels (H_2, methanol, *etc.*). The hydrogen oxidation reaction (HOR) is one of the explored reactions where Pd/CeO_2 proved to be very competitive, taking advantage of the facile Ce^{4+}/Ce^{3+} redox process. The quest for synthetic strategies to maximize the interfacial contact between Pd and CeO_2, which results in higher electrocatalytic activity, is an immediate demonstration of the criticality of the two-component cooperative mechanism.[39] The saturation of CeO_2 with OH^- in alkaline media and their transfer to the metal nanoparticles to form the active $Pd^{I}OH_{ads}$ species is one of the most important catalytic steps for obtaining high HOR activity.[40] However, because of the insulating properties of ceria, the catalyst design must inevitably incorporate conductive phases, typically in the form of carbon black or carbon nanostructures.[41] The resulting interfacial effects in such ternary composites are more complex to analyze, but it is particularly meaningful that the nanostructuring of the composite catalyst allows for improved dispersion and stabilization of the Pd NP on CeO_2. Recently, Ogada *et al.* carried out calculations on the electronic band structures and the projected density of states (PDOS) for nanocomposites where Pd NPs were supported on onion-like carbon (OLC) with and without CeO_2. It turned out that the available states in the CeO_2-free composites were fewer than those in the case of Pd–CeO_2/OLC (Fig. 6). This electronic modulation of Pd by CeO_2 was responsible for the significantly improved performance.[42]

New exploits on PM/CeO_2 catalysts

After decades of research on PM/CeO_2 interaction and synergy, on the catalytic possibilities of such system, above all thermal catalysis but in more recent years also electrocatalysis, it may appear that this particular field has reached complete maturity. Hence, is there still anything to learn? It seems that some work is still devoted to computationally refining some structural details that has been of less interest, but that can still project some effects on catalytic reactions. Monte Carlo simulations have been performed to evaluate the role of the perimeter sites at the Pt/CeO_2 interface during CO oxidation,[43] while DFT combined with first-principles molecular dynamics confirmed the existence of a new class of SMSIs in Pt-SAC/CeO_2 systems, identifying several well-defined and dynamically interconnected charge states originating from the phonon-assisted adjustment of the Ce(4f) level.[44] Other endeavours tackled unexplored synthetic approaches to improve the regulation of the PM–CeO_2 interaction. Plasma irradiation was applied to engineer the surface of CeO_2 nanorods, enhancing the surface roughness and oxygen vacancy content. As a

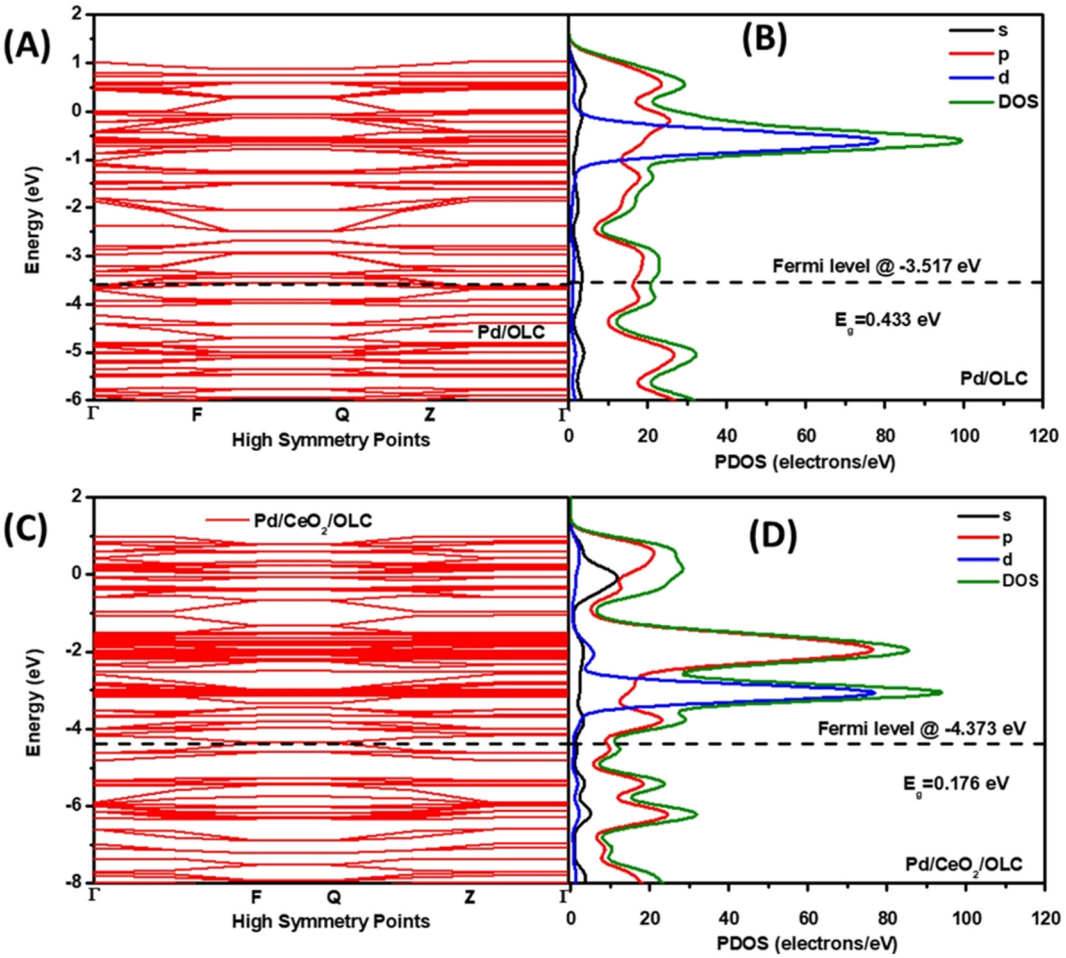

Fig. 6 (A and C) Band structure and (B and D) PDOS of (A and B) Pd/OLC and (C and D) Pd–CeO_2/OLC. Reproduced from ref. 36 with permission from American Chemical Society, copyright 2022.

consequence, they obtain the double advantage of a better dispersion of Pt NPs and an increased amount of extra electrons on the ceria surface, and proposed that the latter effect could reverse the electron transfer between Pt and ceria, with the former exhibiting lower CO chemisorption on account of the higher electron density. The better CO tolerance resulted in higher methanol electro-oxidation activity and stability.[45]

A few years ago, a nanofence structure was assembled by atomic layer deposition (ALD), with CeO_x selectively deposited on Pt(111), which was thus stabilized, leaving Pt(100) exposed and available to catalyse CO oxidation.[46] Despite the large interest in establishing metal–support interfaces in connection with typically observed better catalytic performances, it has been recognised that these systems also suffer from their specific drawbacks. One of these lies in the fact that during long-time operation catalysis, the interface is readily subject to the action of the reactive environment or to an interface reconstruction which alters the properties of the interface and causes loss of catalytic performance, either in terms of activity or selectivity. A recent intriguing opportunity has been offered by the assembly of the so-called "dual-active site" as an alternative configuration of PM/CeO_2 catalysts. In these types of systems, rather than the interface, it is the two different sites (on the metal and on the support) which individually adsorb the two different molecules taking part in the reaction, and activate the overall catalytic process. For example, hydrogenation of nitroarenes was shown to proceed with a cooperative effect between Pd NPs and CeO_2 porous nanorods, whereby the strong adsorption affinity of Pd towards H_2 was flanked by the ability of oxygen vacancy-rich CeO_2 to selectively adsorb the nitroarene. Crucial for the high activity was the sub-nanometric size of the Pd NPs, which disfavoured nitroarene coordination and promoted selective H_2 adsorption.[47] The dual-active site concept was reprised very recently for the reverse water-gas shift reaction (RWGS) by Pt/CeO_2. Here, rather than depending on the metal–support interface, a strong coordination of the CO_2 nanorods was enabled by the presence of frustrated Lewis pairs constructed on the surface of porous CeO_2 nanorods. In parallel, the Pt clusters could readily adsorb and dissociate H_2, finally undergoing H spillover on ceria, where CO_2 was hydrogenated and released CO thanks to its weak interaction with the catalyst.[48]

Very recently, an interesting piece of work addressed the possibility to design smart catalysts based on Pd/CeO_2 where sub-nanometric Pd clusters are able to undergo reversible speciation by means of reactive environment modulation.[49] This is particularly useful for automotive exhaust applications, where differential temperature stages are in place.

In situ and *operando* characterization of the interface

From the latest publications, it is evident that one aspect of growing interest in the realm of PM/CeO_2 catalysts is the necessity to elucidate the role of interfaces under real catalytic conditions. Traditional characterization was usually carried out on bulk materials, fresh or spent catalysts, but the properties so far unravelled have not necessarily been those emerging under real catalytic conditions, where the environment is completely different. Triple (or more) interfaces of varying nature can be formed between the PM, the CeO_2 and the solid, liquid or gaseous reactive mixtures (or a combination of them), requiring specificity of the analytic technique. For example, simulations were used to demonstrate that ceria surfaces behave as proton conductors upon wetting with water, as the water can undergo dissociation into H^+ and OH^- and alter the local pH. The increased local acidity gives rise to a Grotthus-like diffusion mechanism of the ionic species that occurs at the Pt/CeO_2 junction region, and that from there can be channelled along the interface, which has essential repercussions in various applications.[50] In order to probe the dynamic evolution of the multicomponent catalyst in particular at the interfacial sites, and/or understand the adsorption kinetics and thermodynamics of intermediates over the course of the reaction, in the last decade the scene has been dominated by *operando* or *in situ* investigations. In reality, such techniques have been available for more than 20 years,[51] although only scarcely employed, while recent years have witness a

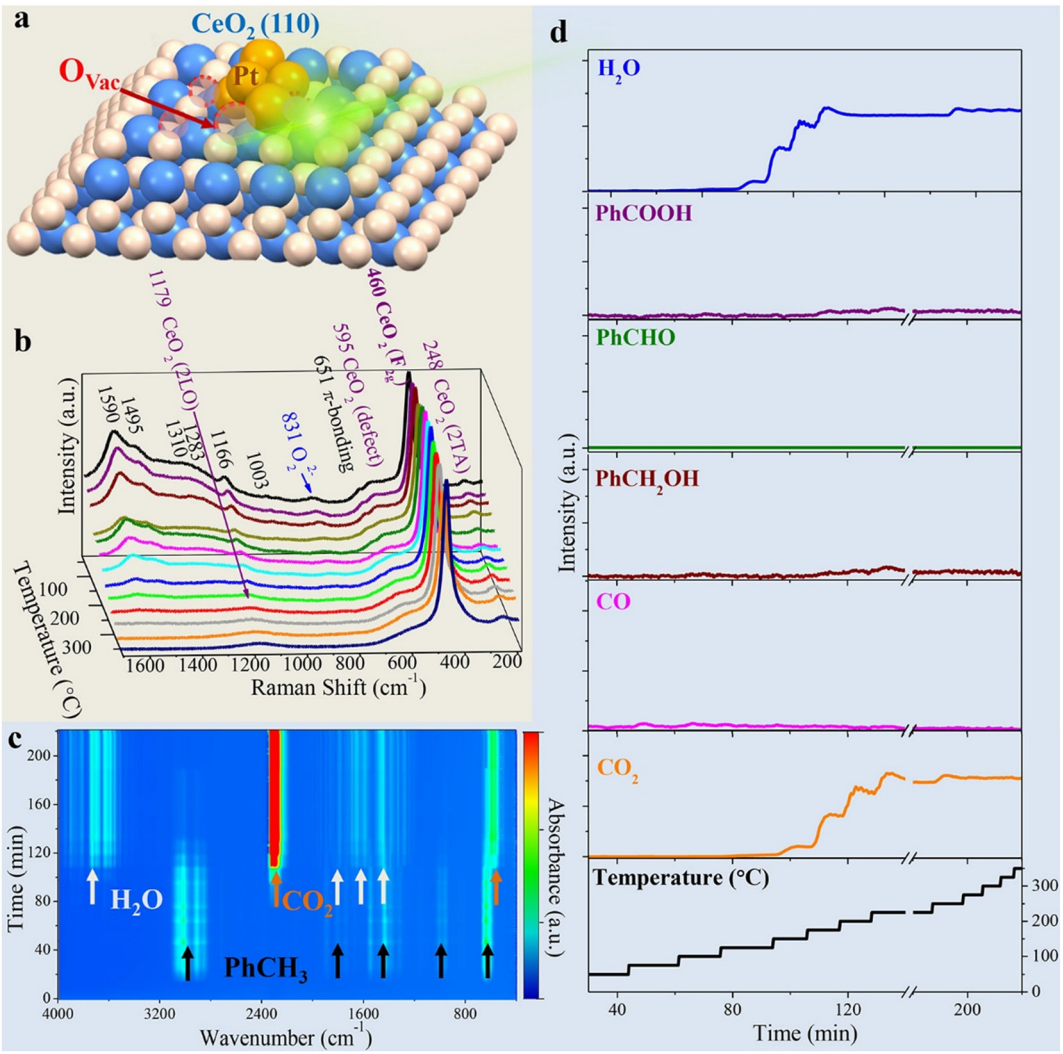

Fig. 7 a) Graphical illustration of the Pt@CeO_2–BDC catalyst with oxygen vacancies (O_{Vac}); b) 3D plot of the *operando* Raman spectra; c) 3D contour plot of the online FTIR spectra; d) plots of reactor temperature program and the corresponding concentration of products. Reproduced from ref. 47 with permission from American Chemical Society, copyright 2021.

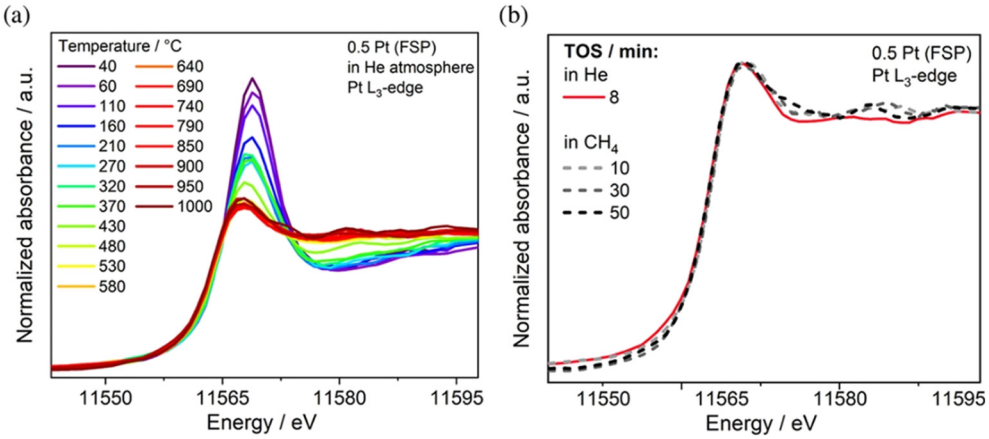

Fig. 8 a) XANES spectra recorded at the Pt L_3-edge of 0.5 Pt (FSP) during heating in He; b) XANES spectra under the reaction at 975 °C in 90% CH_4/He. Reproduced from ref. 50 with permission from American Chemical Society, copyright 2022.

proliferation of articles using them. *In situ* Raman spectroscopy shed some light on the still controversial mechanism of CO oxidation at metal–oxide interfaces. In particular, in the case of CeO_2-based catalysts, the participation of the ceria lattice oxygen is often invoked, as an alternative to the conventional description that the oxidation proceeds merely through superoxide or peroxide species as the active sites. The fabrication of Au@Pt/CeO_2 composites permitted the application of surface-enhanced Raman spectroscopy (SERS), which considerably increased the sensitivity of the technique. Thanks to isotopic substitution experiments it was revealed that much of the activity during CO oxidation originated from chemisorbed Pt–O species at the interfacial Ce^{3+} defect sites, rather than lattice Ce–O species.[52] *Operando* Raman was also used to study toluene oxidation by Pt nanoclusters introduced on MOF-based 1D CeO_2, identifying key intermediates and the role of oxygen vacancies at the Pt/CeO_2 interface (Fig. 7).[53]

A combination of *in situ* Raman and *in situ* diffuse reflectance infrared Fourier transform spectroscopy (DRIFTS) was critical to understand the activity of Au supported on CeO_2 nanorods in the WGSR. Specifically, by comparing Au NPs with smaller size Au nanoclusters, the authors found evidence that the dominating catalytically active species involved a bridged surface –OH group formed at the gold–ceria interface, which explained the considerably higher activity of the nanoclusters.[54] Time-resolved *operando* DRIFTS was used to study the structural evolution of the Au/CO_2 interface in the case of CO oxidation, once again tracing the development of critical carbonate, bicarbonate and formate intermediates at the perimeter of the Au–CeO_2 junction, where $Au^{\delta+}$ was presumed to be formed.[55] The conversion of CH_4 to olefins, aromatic compounds and H_2 catalysed by Pt/CeO_2 has been recently investigated using *operando* X-ray absorption spectroscopy (XAS) in order to unravel the importance of atomically dispersed Pt. It was found that while Pt SACs are active catalysts, aggregated Pt clusters exhibit a comparable activity, thanks to an increased Pt–Ce interaction, which was proposed on the basis of *operando* X-ray absorption near-edge spectroscopy (XANES) during the reaction with CH_4 at 975 °C. The experiments also confirmed a sintering phenomenon of the single site Pt upon heating (Fig. 8).[56]

Recently, Pollastri *et al.* addressed the stability of Pt/CeO_2 catalysts in the context of proton-exchange membrane fuel cells (PEMFC) by means of operando XAS,[57] while Wang *et al.* studied the methanation of CO_2 by Ru/CeO_2 by means of different *in situ* and operando techniques including XANES, Raman and steady-state isotope transient kinetic analysis (SSITKA)-type *in situ* DRIFTS, confirming that the methanation proceeds *via* the formate route with this catalyst.[58] *In situ* electron microscopy has also been used to understand the structural evolution of Pd NPs in a core–shell configuration with CeO_2 during air calcination at different temperatures.[59]

Conclusions and perspectives

The exploitation of PM/CeO_2 interfaces for catalytic applications has enjoyed a great success in the last 30 years, and it seems that it still represents a fertile soil for new discoveries. The primary objective was the stabilization of the PM nanoparticles by the CeO_2 support, which as expected is at the centre of industry's attention for economic reasons, and in general sense for improving the sustainability of catalytic processes. Moreover, stabilization effects take the lead in the case of sub-nanometric PM particles and clusters, and even more in SAC systems, where strong anchoring is critical. However, the role of the interphase between ceria and PMs has revealed its complexity through a large number of research articles, going well beyond the pure structural stabilization of the NP by the support. The dynamics of the PM–ceria "communication" are at times complex, involving electron and/or atom (H spillover), as well as structural alteration of the support structure, predominantly described in terms of oxygen removal. In perspective, such dynamics

will play an important role in those applications where the selectivity of the process is the real goal, such as tandem catalysis or switchable catalysts. Therefore, it clearly emerges that the complexity of the PM/CeO_2 interaction is on the basis of the synergistic PM/CeO_2 catalytic behaviour, and in most cases the synergy originates from the interface region, which coincides with the most active catalytic site. With the advancement of characterization techniques, researchers have been able to ignite ever renewed interest due to new fascinating discoveries and acquired skills to master the synthesis at a notably precise level. Applications have gradually moved from the traditional thermal catalysis to embrace more modern processes of more sustainable nature such as electrocatalysis and, more recently, photocatalysis. As the most abundant rare earth metal, cerium is hardly to be replaced in the design of catalytic nanocomposites, given the exclusive redox behaviour of rare earth metal oxides. On the other hand, efforts for more sustainable materials may be directed in the replacement of PMs with more abundant transition metals. A large number of notable reports are already available where some catalytic reactions can transcend PM active metals and resort instead to other readily available metals exhibiting interfacial effects, obtaining an overall high efficiency.[60] New paradigms are continuously established, and much of the merits are derived from ingenious strategies to alter catalyst structures with innovative methodologies, although the presence of the metal–ceria interface always remains the cornerstone. After many years of studying ceria-based catalysts, our feeling is that much is yet to come.

Conflicts of interest

There are no conflicts to declare.

Acknowledgements

This work was supported by the University of Trieste, INSTM, the European Commission (H2020 – RIA-CE-NMBP-25 Program, Grant No. 862030). We acknowledge the COST Action 21101. M. M. acknowledges the project P2022WANKS funded by the Ministero dell'Università e della Ricerca (MUR) and the project FRA2022 funded by the University of Trieste.

References

1 E. B. Maxted and S. Akhtar, *J. Chem. Soc.*, 1960, 1995–1998.
2 (*a*) L. Mendelovich, H. Tzehoval and M. Steinberg, *Appl. Surf. Sci.*, 1983, **17**, 175–188; (*b*) D. W. Daniel, *J. Phys. Chem.*, 1988, **92**, 3891–3899; (*c*) J. Z. Shyu and K. Otto, *J. Catal.*, 1989, **115**, 16–23.
3 (*a*) B. Engler, E. Koberstein and P. Schubert, *Appl. Catal.*, 1989, **48**, 71–92; (*b*) G. Kim, *Ind. Eng. Chem. Prod. Res. Dev.*, 1982, **21**, 267–274.
4 (*a*) J. Kašpar, P. Fornasiero and M. Graziani, *Catal. Today*, 1999, **50**, 285–298; (*b*) J. Kašpar, P. Fornasiero and N. Hickey, *Catal. Today*, 2003, **77**, 419–449.
5 T. Montini, M. Melchionna, M. Monai and P. Fornasiero, *Chem. Rev.*, 2016, **116**, 5987–6041.
6 (*a*) T. Bunluesin, R. J. Gorte and G. W. Graham, *Appl. Catal., B*, 1998, **15**, 107–114; (*b*) A. Trovarelli, *Catal. Rev.: Sci. Eng.*, 1996, **38**, 439–520.
7 M. Cargnello, J. J. D. Jaén, J. C. H. Garrido, K. Bakhmutsky, T. Montini, J. J. C. Gámez, R. J. Gorte and P. Fornasiero, *Science*, 2012, **337**, 713–717.
8 M. Cargnello, P. Fornasiero and R. J. Gorte, *Catal. Lett.*, 2012, **142**, 1043–1048.
9 F. Esch, S. Fabris, L. Zhou, T. Montini, C. Africh, P. Fornasiero, G. Comelli and R. Rosei, *Science*, 2005, **309**, 752–755.
10 S. J. Tauster, S. C. Fung and R. L. Garten, *J. Am. Chem. Soc.*, 1978, **100**, 170–175.
11 M. G. Sanchez and J. L. Gazquez, *J. Catal.*, 1987, **104**, 120–135.
12 (*a*) S. Bernal, J. J. Calvino, M. A. Cauqui, G. A. Cifredo, A. Jobacho and J. M. Rodríguez-Izquierdo, *Appl. Catal., A*, 1993, **99**, 1–8; (*b*) S. Bernal, J. J. Calvino, M. A. Cauqui, J. A. Pérez Omil, J. M. Pintado and J. M. Rodríguez-Izquierdo, *Appl. Catal., B*, 1998, **16**, 127–138; (*c*) S. Bernal, J. J. Calvino, M. A. Cauqui, J. M. Gatica, C. Larese, J. A. Pérez Omil and J. M. Pintado, *Catal. Today*, 1999, **50**, 175–206.
13 J. C. Frost, *Nature*, 1988, **334**, 577–580.
14 N. Acerbi, S. C. Tsang, S. Golunski and P. Collier, *Chem. Commun.*, 2008, 1578–1580.
15 N. Acerbi, S. C. E. Tsang, G. Jones, S. Golunski and P. Collier, *Angew. Chem., Int. Ed.*, 2013, **52**, 7737–7741.
16 (*a*) A. Trovarelli, C. de Leitenburg and G. Dolcetti, *J. Chem. Soc., Chem. Commun.*, 1991, 472–473; (*b*) C. Deleitenburg and A. Trovarelli, *J. Catal.*, 1995, **156**, 171–174.
17 A. Trovarelli, C. Deleitenburg, G. Dolcetti and J. L. Lorca, *J. Catal.*, 1995, **151**, 111–124.
18 S. Li, Y. Xu, Y. Chen, W. Li, L. Lin, M. Li, Y. Deng, X. Wang, B. Ge, C. Yang, S. Yao, J. Xie, Y. Li, X. Liu and D. Ma, *Angew. Chem., Int. Ed.*, 2017, **56**, 10761–10765.
19 N. C. Nelson, J. S. Manzano, A. D. Sadow, S. H. Overbury and I. I. Slowing, *ACS Catal.*, 2015, **5**, 2051–2061.
20 C. T. Campbell, *Nat. Chem.*, 2012, **4**, 597–598.
21 A. Bruix, J. A. Rodriguez, P. J. Ramírez, S. D. Senanayake, J. Evans, J. B. Park, D. Stacchiola, P. Liu, J. Hrbek and F. Illas, *J. Am. Chem. Soc.*, 2012, **134**, 8968–8974.
22 (*a*) C. Hardacre, G. M. Roe and R. M. Lambert, *Surf. Sci.*, 1995, **326**, 1–10; (*b*) U. Berner and K.-D. Schierbaum, *Phys. Rev. B*, 2002, **65**, 235404.
23 (*a*) P. Luches and S. Valeri, *Materials*, 2015, **8**, 5818–5833; (*b*) P. Luches, F. Pagliuca and S. Valeri, *J. Phys. Chem. C*, 2011, **115**, 10718–10726; (*c*) P. Luches, F. Pagliuca and S. Valeri, *Phys. Chem. Chem. Phys.*, 2014, **16**, 18848–18857.
24 J. A. Rodriguez, D. C. Grinter, Z. Liu, R. M. Palomino and S. D. Senanayake, *Chem. Soc. Rev.*, 2017, **46**, 1824–1841.
25 (*a*) D. C. Grinter, C. L. Pang, C. A. Muryn, F. Maccherozzi, S. S. Dhesi and G. Thornton, *J. Electron Spectrosc. Relat. Phenom.*, 2014, **195**, 13–17; (*b*) B. Kaemena, S. D. Senanayake, A. Meyer, J. T. Sadowski, J. Falta and J. I. Flege,

J.Phys. Chem. C, 2013, **117**, 221–232; (*c*) J. I. Flege and D. C. Grinter, *Prog. Surf. Sci.*, 2018, **93**, 21–45.

26 S. D. Senanayake, D. Stacchiola and J. A. Rodriguez, *Acc. Chem. Res.*, 2013, **46**, 1702–1711.

27 W. C. Conner, Jr. and J. L. Falconer, *Chem. Rev.*, 1995, **95**, 759–788.

28 F. Yang, J. Graciani, J. Evans, P. Liu, J. Hrbek, J. F. Sanz and J. A. Rodriguez, *J. Am. Chem. Soc.*, 2011, **133**, 3444–3451.

29 P. Luches, G. Gasperi, M. Sauerbrey, S. Valeri, J. Falta and J. I. Flege, *Front. Chem.*, 2019, 7.

30 (*a*) A. Beltram, M. Melchionna, T. Montini, L. Nasi, R. J. Gorte, M. Prato and P. Fornasiero, *Catal. Today*, 2015, **253**, 142–148; (*b*) M. Melchionna, A. Beltram, A. Stopin, T. Montini, R. W. Lodge, A. N. Khlobystov, D. Bonifazi, M. Prato and P. Fornasiero, *Appl. Catal., B*, 2018, **227**, 356–365; (*c*) G. Valenti, M. Melchionna, T. Montini, A. Boni, L. Nasi, E. Fonda, A. Criado, A. Zitolo, S. Voci, G. Bertoni, M. Bonchio, P. Fornasiero, F. Paolucci and M. Prato, *ACS Appl. Energy Mater.*, 2020, **3**, 8509–8518.

31 X. Zhang, D. Zhou, X. Wang, J. Zhou, J. Li, M. Zhang, Y. Shen, H. Chu and Y. Qu, *ACS Catal.*, 2020, **10**, 3832–3837.

32 Q. Fu, H. Saltsburg and M. Flytzani-Stephanopoulos, *Science*, 2003, **301**, 935–938.

33 Y. Zhai, D. Pierre, R. Si, W. Deng, P. Ferrin, A. U. Nilekar, G. Peng, J. A. Herron, D. C. Bell, H. Saltsburg, M. Mavrikakis and M. Flytzani-Stephanopoulos, *Science*, 2010, **329**, 1633–1636.

34 (*a*) M. Yang, S. Li, Y. Wang, J. A. Herron, Y. Xu, L. F. Allard, S. Lee, J. Huang, M. Mavrikakis and M. Flytzani-Stephanopoulos, *Science*, 2014, **346**, 1498–1501; (*b*) M. Yang, J. Liu, S. Lee, B. Zugic, J. Huang, L. F. Allard and M. Flytzani-Stephanopoulos, *J. Am. Chem. Soc.*, 2015, **137**, 3470–3473.

35 L. Nie, D. Mei, H. Xiong, B. Peng, Z. Ren, X. I. P. Hernandez, A. DeLaRiva, M. Wang, M. H. Engelhard, L. Kovarik, A. K. Datye and Y. Wang, *Science*, 2017, **358**, 1419–1423.

36 C. Wang, X.-K. Gu, H. Yan, Y. Lin, J. Li, D. Liu, W.-X. Li and J. Lu, *ACS Catal.*, 2017, **7**, 887–891.

37 O. A. Marina and M. Mogensen, *Appl. Catal., A*, 1999, **189**, 117–126.

38 (*a*) K. Kwon, K. H. Lee, S.-A. Jin, D. J. You and C. Pak, *Electrochem. Commun.*, 2011, **13**, 1067–1069; (*b*) D.-H. Lim, W.-D. Lee, D.-H. Choi and H.-I. Lee, *Appl. Catal., B*, 2010, **94**, 85–96.

39 H. A. Miller, M. Bellini, D. R. Dekel and F. Vizza, *Electrochem. Commun.*, 2022, **135**, 107219.

40 H. A. Miller, A. Lavacchi, F. Vizza, M. Marelli, F. Di Benedetto, F. D'Acapito, Y. Paska, M. Page and D. R. Dekel, *Angew. Chem., Int. Ed.*, 2016, **55**, 6004–6007.

41 (*a*) A. Lenarda, M. Bellini, A. Marchionni, H. A. Miller, T. Montini, M. Melchionna, F. Vizza, M. Prato and P. Fornasiero, *Inorg. Chim. Acta*, 2018, **470**, 213–220; (*b*) R. K. Singh, E. S. Davydova, J. Douglin, A. O. Godoy, H. Tan, M. Bellini, B. J. Allen, J. Jankovic, H. A. Miller, A. C. Alba-Rubio and D. R. Dekel, *Adv. Funct. Mater.*, 2020, **30**, 2002087.

42 J. J. Ogada, A. K. Ipadeola, P. V. Mwonga, A. B. Haruna, F. Nichols, S. Chen, H. A. Miller, M. V. Pagliaro, F. Vizza, J. R. Varcoe, D. M. Meira, D. M. Wamwangi and K. I. Ozoemena, *ACS Catal.*, 2022, **12**, 7014–7029.

43 N. Bosio, M. Di, M. Skoglundh, P.-A. Carlsson and H. Grönbeck, *J. Phys. Chem. C*, 2022, **126**, 16164–16171.

44 N. Daelman, M. Capdevila-Cortada and N. López, *Nat. Mater.*, 2019, **18**, 1215–1221.

45 L. Tao, Y. Shi, Y.-C. Huang, R. Chen, Y. Zhang, J. Huo, Y. Zou, G. Yu, J. Luo, C.-L. Dong and S. Wang, *Nano Energy*, 2018, **53**, 604–612.

46 K. Cao, L. Shi, M. Gong, J. Cai, X. Liu, S. Chu, Y. Lang, B. Shan and R. Chen, *Small*, 2017, **13**, 1700648.

47 S. Zhang, C.-R. Chang, Z.-Q. Huang, J. Li, Z. Wu, Y. Ma, Z. Zhang, Y. Wang and Y. Qu, *J. Am. Chem. Soc.*, 2016, **138**, 2629–2637.

48 W. Li, J. Gan, Y. Liu, Y. Zou, S. Zhang and Y. Qu, *Angew. Chem., Int. Ed.*, 2023, **62**, e202305661.

49 D. Jiang, G. Wan, J. Halldin Stenlid, C. E. García-Vargas, J. Zhang, C. Sun, J. Li, F. Abild-Pedersen, C. J. Tassone and Y. Wang, *Nat. Catal.*, 2023, **6**, 618–627.

50 M. Farnesi Camellone, F. Negreiros Ribeiro, L. Szabová, Y. Tateyama and S. Fabris, *J. Am. Chem. Soc.*, 2016, **138**, 11560–11567.

51 G. Jacobs, P. M. Patterson, L. Williams, E. Chenu, D. Sparks, G. Thomas and B. H. Davis, *Appl. Catal., A*, 2004, **262**, 177–187.

52 D.-Y. Wei, M.-F. Yue, S.-N. Qin, S. Zhang, Y.-F. Wu, G.-Y. Xu, H. Zhang, Z.-Q. Tian and J.-F. Li, *J. Am. Chem. Soc.*, 2021, **143**, 15635–15643.

53 Q. Wang, Y. Li, A. Serrano-Lotina, W. Han, R. Portela, R. Wang, M. A. Bañares and K. L. Yeung, *J. Am. Chem. Soc.*, 2021, **143**, 196–205.

54 X.-P. Fu, L.-W. Guo, W.-W. Wang, C. Ma, C.-J. Jia, K. Wu, R. Si, L.-D. Sun and C.-H. Yan, *J. Am. Chem. Soc.*, 2019, **141**, 4613–4623.

55 S. Chen, L. Luo, Z. Jiang and W. Huang, *ACS Catal.*, 2015, **5**, 1653–1662.

56 D. Eggart, X. Huang, A. Zimina, J. Yang, Y. Pan, X. Pan and J.-D. Grunwaldt, *ACS Catal.*, 2022, **12**, 3897–3908.

57 S. Pollastri, M. Bogar, R. Fiala, H. Amenitsch, Y. Yakovlev, A. Lavacchi, G. Aquilanti and V. Matolin, *Int. J. Hydrogen Energy*, 2022, **47**, 8799–8810.

58 F. Wang, S. He, H. Chen, B. Wang, L. Zheng, M. Wei, D. G. Evans and X. Duan, *J. Am. Chem. Soc.*, 2016, **138**, 6298–6305.

59 S. Zhang, C. Chen, M. Cargnello, P. Fornasiero, R. J. Gorte, G. W. Graham and X. Pan, *Nat. Commun.*, 2015, **6**, 7778.

60 (*a*) A. Parastaev, V. Muravev, E. Huertas Osta, A. J. F. van Hoof, T. F. Kimpel, N. Kosinov and E. J. M. Hensen, *Nat. Catal.*, 2020, **3**, 526–533; (*b*) A. Chen, X. Yu, Y. Zhou, S. Miao, Y. Li, S. Kuld, J. Sehested, J. Liu, T. Aoki, S. Hong, M. F. Camellone, S. Fabris, J. Ning, C. Jin, C. Yang, A. Nefedov, C. Wöll, Y. Wang and W. Shen, *Nat. Catal.*, 2019, **2**, 334–341; (*c*) Y. Wang, Q. Jiang, L. Xu, Z.-K. Han, S. Guo, G. Li and A. Baiker, *ACS Appl. Mater. Interfaces*, 2021, **13**, 61078–61087.